Distribution Network Operation by Coordination of Flexible Loads, SOP, and Smart Transformer

Alok Kumar
Department of Electrical Engineering
Indian Institute of Technology (BHU)
Varanasi, India
alok.kumar1@live.com

Avirup Maulik
Department of Electrical Engineering
Indian Institute of Technology (BHU)
Varanasi, India
avirupmaulik@gmail.com

K. A. Chinmaya
Department of Electrical Engineering
Indian Institute of Technology (BHU)
Varanasi, India
chinmay.vasista@gmail.com

***Abstract*—The penetration of embedded generation, including renewable power sources (wind and solar), is gradually increasing in power distribution networks. Also, the transition from conventional fossil fuel-based transportation to e-transportation has introduced electric vehicle charging stations as a new load class. The conventional distribution system architecture alteration has made the system operation rather challenging. Therefore, an efficient energy management scheme is crucial to the satisfactory operation of an active distribution system from techno-economic considerations. This paper proposes an optimal operating strategy to simultaneously minimize the operating cost, average voltage deviation, and line loadings and improve the voltage stability of an active distribution network. The distribution system is assumed to have a soft open point and smart transformer for smooth active and reactive power control. The demand response flexibility (offered by responsive electrical demands and public and residential electric vehicle charging stations) is coordinated by controlling a smart transformer and a soft open point to realize multiple objectives. The multi-objective problem is solved in the fuzzy domain using a combination of linear programming and particle swarm optimization. Simulation results on a sixty-nine-bus radial distribution system validate the proposed method's effectiveness.**

***Index Terms*—Electric Vehicles, Renewable Energy, Demand Response, Soft Open Points, Particle Swarm Optimization, Smart Transformer.**

I. Introduction

With the increasing integration of distributed energy resource (DER) and electric vehicle (EV), the operation of an active distribution network has become challenging. The distribution network operator (DNO) can compensate for the renewable energy source (RES) generation and EV load variability by demand response (DR) implementation or by using distributed battery energy storage system (DBESS). Further, power electronic devices like the soft open point (SOP) and smart transformer (ST) allow smooth control of active and reactive power and automation of a distribution system [1]. Therefore, DR has the potential to ensure grid security and increase the efficiency of the power network. In this context, an effective energy management scheme (EMS) is needed for the satisfactory operation of a distribution system from a techno-economic viewpoint.

The DR participation is ensured through price or incentive-based options. A data-driven incentive-based DR was formulated in a robust optimization framework to address the uncertainties from the load demands, renewable energy generations, and DR resources [2]. A tri-level two-stage price-based demand response (PBDR) in a non-cooperative game theoretic framework using a two-loop Stackelberg game is proposed [3]. A coordinated optimization scheme for incorporating battery energy storage system (BESS) and SOP in combined DR and conservation voltage reduction (CVR) scheme is presented in [4]. A two-stage stochastic optimization with integrated DR is proposed for community integrated energy system (CIES) to schedule various energy equipment following the changes in user demand patterns and energy prices [5]. Recent studies reveal that an SOP in coordination with DR can reduce the active power losses, increasing voltage stability index (VSI), reducing average voltage deviation (AVD), decreasing the line loading, and ultimately enhancing hosting capacity (HC) of a distributions system [6]. A two-layer control strategy is proposed using an SOP in the form of load regulation considering the economic operation area of the transformers and peer-to-peer control of each port to suppress the voltage fluctuation [7]. A multi-objective probabilistic EMS is proposed to simultaneously reduce the cost of operation, improve the voltage profile, and minimize AVD in a distribution network considering SOP [8]. A multi-time scale EMS framework has been proposed using for multi-terminal SOP-based active distribution network (ADN) considering Stackelberg theoretic game relationship between the ADN and microgrids [9].

This paper proposes a multi-objective EMS for simultaneous cost minimization, VSI improvement, AVD minimization, and minimization of line current loading in a power distribution network considering RES and plug-in electric vehicle (PEV) loads. The multi-objective multi-constraint optimization problem has been solved using particle swarm optimization (PSO). The remainder of this paper is arranged as follows. Mathematical modelling is presented in section II, solution approach in section III, and simulation studies in section IV followed by conclusions in section V.

II. Mathematical modeling

The distribution network comprises RES (i.e., solar photovoltaic generation system (SPGS) and wind power generation system (WPGS)), electrical loads, an SOP, residential and public electric vehicle charging station (EVCS). A fraction of the electrical loads, residential and public EVCSs participate in the DR program and provide flexibility to the distribution system operator (DSO). A ST interfaces the distribution network with the upstream grid. The distribution network is further equipped with an SOP. The ST and SOP offer further flexibility in the distribution network operation. The DSO gathers information about the hourly grid power price and the price of DR participation from the day-ahead energy

market. An optimal EMS is followed by the DSO to reduce the total cost of operation, improve the voltage stability, reduce the AVD, and reduce the line loadings. The objective values are of different orders. Therefore, each objective is normalized by assigning a fuzzy membership function (FMF). The maximum value of a FMF is 1, which denotes complete satisfaction of the objective. On the other hand, the minimum value of the FMF is 0 and denotes non-satisfaction of the objective. A high value of the FMF signifies the attainment of the objective to a greater extent. The multi-objective multi-constraint optimization problem is described below.

A. Objective functions

Each objective function is described below:

1) Reduction of total operating cost: The total cost of operation (κ) is given by :

$$\kappa = \sum_{t\in\Omega_t} \kappa^t = \sum_{t\in\Omega_t} \lambda_g^t P_g^t + \lambda_{dr}^t \sum_{m2\in\omega_b} ((P_l^{0t}(m2) + P_{rev}^{0t}(m2) + P_{pev}^{0t}(m2)) - (P_l^t(m2) + P_{rev}^t(m2) + P_{pev}^t(m2))) \quad (1)$$

The first term on the right hand side (RHS) of (1) denotes the cost of energy drawn from the grid, while the second term denotes the price of DR implementation. t denotes a time window (taken as one hour in this paper), and Ω_t is the set of all one-hour windows under consideration (taken as 24 hours for a day). Superscript t denotes the value of a variable at time t. λ_g^t denotes the price of electricity procured from the grid, P_g^t denotes the power imported from the main grid, and λ_{dr}^t denotes the DR price for the time slot t. P_l^t/P_l^{0t} denotes the load demand after/before implementation of the DR program during the time window t. P_{rev}^t/P_{rev}^{0t} denotes the residential EV's load demand after/before implementation of the DR program during the time window t. P_{pev}^t/P_{pev}^{0t} denotes the public EV's load demand after/before implementation of the DR program during the time window t. $m2$ denotes a bus in the system, and Ω_b is the set of all system buses. The following FMF is assigned to the objective ($t \in \Omega_t$):

$$\mu_1^t = \begin{cases} \frac{\kappa_{max}^t - \kappa^t}{\kappa_{max}^t - \kappa_{min}^t} & : \kappa_{min}^t \le \kappa^t \le \kappa_{max}^t \\ 1 & : \kappa^t < \kappa_{min}^t \\ 0 & : \kappa^t > \kappa_{max}^t \end{cases} \quad (2)$$

where κ_{max}^t and κ_{min}^t are upper and lower thresholds of κ^t. The FMF attains the maximum value of 1 when $\kappa^t \le \kappa_{min}^t$, and the minimum value of 0 when $\kappa^t \ge \kappa_{max}^t$. The value of the FMF decreases linearly in between. Therefore, reducing the total operating cost will lead to a higher value of the FMF.

2) Improvement of VSI: The VSI of a bus $m2$ ($\upsilon^t(m2)$) in a radial distribution network is computed by [10]:

$$\upsilon^t(m2) = (|V^t(m1)|^4 - 4(P^t(m2)x_l - Q^t(m2)r_l)^2 - 4(P^t(m2)r_l - Q^t(m2)x_l))(|V^t(m1)|)^2 \quad (3)$$

where $m1$ and $m2$ denote the sending and receiving end buses of line l having resistance and reactance values of r_l and x_l, respectively. $P(m2)$ and $Q(m2)$ denote the total active and reactive powers fed through the bus $m2$. $|V(m2/m1)|$ is the voltage magnitude at bus $m2/m1$. In this paper, the objective is to maximize the VSI of the most vulnerable bus, i.e., to maximize the minimum value of the VSI (ν^t) as given below:

$$\nu^t = \min_{m2}\{\upsilon^t(m2)\} \quad m2 \in \Omega_b \setminus 1 \quad (4)$$

Ω_b denotes the set of all buses. The objective is to improve the value of VSI, i.e., a higher value of VSI should yield a higher value of the FMF. Therefore, the following FMF is assigned:

$$\mu_2^t = \begin{cases} \frac{\nu^t - \nu_{min}^t}{\nu_{max}^t - \nu_{min}^t} & : \nu_{min}^t \le \nu^t \le \nu_{max}^t \\ 0 & : \nu^t < \nu_{min}^t \\ 1 & : \nu^t > \nu_{max}^t \end{cases} \quad (5)$$

where ν_{max}^t and ν_{min}^t are upper and lower thresholds of ν^t

3) Reduction of AVD: The AVD (η^t) in a network is given as follows :

$$\eta^t = \frac{1}{\#\Omega_b} \sum_{b\in\Omega_b} |(1.0 - |V^t(b)|)| \quad (6)$$

The ideal/nominal voltage magnitude is considered as 1.0 p.u. in this paper. Since the objective is to reduce the AVD a FMF similar to that assigned in section II-A1 is assigned:

$$\mu_3^t = \begin{cases} \frac{\eta_{max}^t - \eta^t}{\eta_{max}^t - \eta_{min}^t} & : \eta_{min}^t \le \eta^t \le \eta_{max}^t \\ 1 & : \eta^t < \eta_{min}^t \\ 0 & : \eta^t > \eta_{max}^t \end{cases} \quad (7)$$

where η_{max}^t and η_{min}^t are upper and lower thresholds of η^t.

4) Reduction of line loading: Integration of EV load and RES can lead to feeder overloads. Therefore, an important objective is to minimize feeder loadings. In this paper, the objective is to minimize the percentage loading of the most heavily loaded feeder (ψ^t) as given below:

$$\psi^t = \max_l\{\frac{|I^t(l)|}{I^{rat}(l)} \times 100\} \quad l \in \Omega_l \quad (8)$$

where $|I(l)|$ and $|I^{rat}(l)|$ denote the actual and the rated current magnitudes of line l, respectively. Ω_l denotes the set of all feeders. Since this objective is to be minimized, the following FMF is allocated:

$$\mu_4^t = \begin{cases} \frac{\psi_{max}^t - \psi^t}{\psi_{max}^t - \psi_{min}^t} & : \psi_{min}^t \le \psi^t \le \psi_{max}^t \\ 1 & : \psi^t < \psi_{min}^t \\ 0 & : \psi^t > \psi_{max}^t \end{cases} \quad (9)$$

5) Combined objective: Multi-objective optimization involves simultaneously attaining multiple goals and finding a trade-off solution. If the i^{th} objective is only considered in the EMS, then $\mu_i = 1.0$. Therefore, the utopian point is 1.0 for each objective. The trade-off solution in this paper is obtained by minimizing the Euclidian distance to utopia points for each objective as given below [11]:

$$\min \Delta^t = \sqrt{\sum_{i=1}^{4}(1-\mu_i)^2} \quad : i = \{1,2,3,4\} \quad (10)$$

B. Constraints

The system constraints are as follows:

$$P_s^t(m1) + P_w^t(m1) + P_{sop}^t(m1) - (P_l^t(m1) + P_{rev}^t(m1) + P_{pev}^t(m1)) = |V^t(m1)| \sum_{m2\in\Omega_b} |V^t(m2)||Y(m1)(m2)|cos(\delta^t(m1) - \delta^t(m2) - \theta^t(m1)(m2)) \quad : m1 \in \Omega_b \setminus 1; m2 \in \Omega_b \tag{11}$$

$$Q_s^t(m1) + Q_w^t(m1) + Q_{sop}^t(m1) - (Q_l^t(m1) + Q_{rev}^t(m1) + Q_{pev}^t(m1)) = |V^t(m1)| \sum_{m2\in\Omega_b} |V^t(m2)||Y(m1)(m2)|sin(\delta^t(m1) - \delta^t(m2) - \theta^t(m1)(m2)) \quad : m1 \in \Omega_b \setminus 1; m2 \in \Omega_b \tag{12}$$

$$P_g^t = |V^t(1)| \sum_{m2\in\Omega_b} (|V^t(m2)||Y(1)(m2)|cos(\delta^t(1) - \delta^t(m2) - \theta^t(1)(m2))) \quad : m2 \in \Omega_b \tag{13}$$

$$Q_g^t = |V^t(1)| \sum_{m2\in\Omega_b} (|V^t(m2)||Y(1)(m2)|sin(\delta^t(1) - \delta^t(m2) - \theta^t(1)(m2))) \quad : m2 \in \Omega_b \tag{14}$$

Algorithm 1: Algorithm for optimization

```
/* Stage 1-Solve using Linear
   Programming                                  */
```
Data: $P_l^{0t}(m2)$, $P_{rev}^{0t}(m2)$, $P_{pev}^{0t}(m2)$, λ_g^t, λ_{dr}^t $t \in \Omega_t, m2 \in \Omega_b$

$\min \kappa$ s.t (19) and (20)

Result: $P_l^t(m2)$, $P_{rev}^t(m2)$, $P_{pev}^t(m2)$ $t \in \Omega_t, m2 \in \Omega_b$

```
/* Stage 2-Solve using PSO                     */
```
Data: Result from stage 1, network data, SOP, ST data

Set $t = 1$; **while** $t \leq 24$ **do**

  Set $i = 1$;**while** $i \leq 4$ **do**

    if $i = 1$ **then**

      Obj: $\min \kappa^t$ s.t. constraints

    else if $i = 2$ **then**

      Obj: $\max \nu^t$ s.t. constraints

    else if $i = 3$ **then**

      Obj: $\min \eta^t$ s.t. constraints

    else

      Obj: $\min \psi^t$ s.t. constraints

    Use PSO to optimize; record all objective values;

  /* Finding lower and upper bounds of objectives */

  $\kappa_{min}^t = \min_i \kappa^t$; $\kappa_{max}^t = \max_i \kappa^t$;

  $\nu_{min}^t = \min_i \nu^t$; $\nu_{max}^t = \max_i \nu^t$;

  $\eta_{min}^t = \min_i \eta^t$; $\eta_{max}^t = \max_i \eta^t$;

  $\psi_{min}^t = \min_i \psi^t$; $\psi_{max}^t = \max_i \psi^t$;

  Run PSO to $\min \Delta^t$ s.t. constraints ; // Use upper & lower bounds of objectives for FMF

  Result: $P_{sop}^t(m1)$, $Q_{sop}^t(m1)$, $Q_{sop}^t(m2)$, $|V(1)^t|$

$$|I^t(l)| \leq |I^{rat}(l)| \quad : t \in \Omega_t; l \in \Omega_l \tag{15}$$

$$|V_{min}^t| \leq |V^t(m2)| \leq |V_{max}^t| \quad : t \in \Omega_t; m2 \in \Omega_b \tag{16}$$

$$\sqrt{(P_g^t)^2 + (Q_g^t)^2} \leq S_{stmax} \tag{17}$$

$$0.95 \leq |V^t(1)| \leq 1.05 \quad t \in \Omega_t \tag{18}$$

$$\begin{cases} \sum_{t\in\Omega_t} P_l^t(m2) = \sum_{t\in\Omega_t} P_l^{0t}(m2) & m2 \in \Omega_b \setminus 1 \\ \sum_{t\in\Omega_t} P_{rev}^t(m2) = \sum_{t\in\Omega_t} P_{rev}^{0t}(m2) & m2 \in \Omega_b \setminus 1 \\ \sum_{t\in\Omega_t} P_{pev}^t(m2) = \sum_{t\in\Omega_t} P_{pev}^{0t}(m2) & m2 \in \Omega_b \setminus 1 \end{cases} \tag{19}$$

$$\begin{cases} (1-\lambda_l^t)P_l^{0t}(m2) \leq P_l^t(m2) \leq (1+\lambda_l^t)P_l^{0t}(m2) \\ (1-\lambda_{rev}^t)P_{rev}^{0t}(m2) \leq P_{rev}^t(m2) \leq (1+\lambda_{rev}^t)P_{rev}^{0t}(m2) \\ (1-\lambda_{pev}^t)P_{pev}^{0t}(m2) \leq P_{pev}^t(m2) \leq (1+\lambda_{pev}^t)P_{pev}^{0t}(m2) \end{cases} \tag{20}$$

$$P_{sop}^t(m1) + (1-k_{sop})P_{sop}^t(m2) = 0 : (m1, m2) \in \Omega_{sop(\zeta)} \tag{21}$$

$$\sqrt{(P_{sop}^t(m1))^2 + (Q_{sop}^t(m1))^2} \leq S_{sop}(m1) \tag{22}$$

$$\sqrt{(P_{sop}^t(m2))^2 + (Q_{sop}^t(m2))^2} \leq S_{sop}(m2) \tag{23}$$

The active and reactive power balances at system buses, including the substation bus are given by (11), (12), (13), and (14). $P_s(m1)$/$Q_s(m1)$, $P_w(m1)$/$Q_w(m1)$, and $P_{sop}(m1)$/$Q_{sop}(m1)$ denote the active/reactive powers injected at bus $m1$ by SPGS, WPGS, and SOP, respectively. The magnitude and angle of the element in the $m1^{th}$ row and $m2^{th}$ column are given by $Y(m1)(m2)$ and $\theta(m1)(m2)$, respectively. $\delta(m1)$ denotes the voltage angle of the $m1^{th}$ bus. P_g and Q_g denote the active and reactive power injection to the distribution network from the load side converter of the ST. The current rating constraint of a feeder is given by (15). The bus voltage constraint is given by (16). $|V_{min}|$ and $|V_{max}|$ denote the minimum and maximum allowable limits, respectively. The apparent power rating constraint of the ST is given by (17). S_{stmax} is the apparent power rating of the load side converter of the ST. (18) denotes that the voltage setting of the load side converter of the ST can be set between 0.95 p.u. and 1.05 p.u. (19) denotes that the energy of responsive/flexible loads (electrical, residential EV, and public EV) cannot be curtailed over a day; they can only be shifted. (20) states that the shift of responsive loads should be within given limits. λ_l, λ_{pev}, and λ_{rev} denote the limits of shiftable responsible loads for different customers (electrical loads, residential EV and public EV charging loads). The power balance equation of an SOP ζ is given by (21). The loss factor of the SOP is denoted by k_{sop}. Ω_{sop} denotes the set of SOPs in the network. The apparent power constraint of the SOP is given by (22) and (23). The apparent power rating of the voltage source converter of the SOP connected to bus $m1$ is given by $S_{sop}(m1)$.

III. Solution approach

The problem is solved in two stages. In stage 1, the DR is implemented using linear programming. The following optimization problem is solved:

$$\min \kappa \tag{24}$$

s.t. (19) and (20). P_g^t is computed by neglecting the system loss at this stage (i.e., P_g^t is found by subtracting the total effective generation of RES from the total effective load (i.e., electrical loads, residential EV, and commercial EV). The control variables $\Xi = \{P_l^t, P_{rev}^t, P_{pev}^t\}$. The optimization problem is solved using the "linprog" toolbox of MATLAB. The optimal setting of $\{P_l^t, P_{rev}^t, P_{pev}^t\}$ are fed to stage 2.

Stage 2 of the optimization program uses PSO to optimize the settings of the SOP and ST. Therefore, the control variables are $\Xi = \{P_{sop}^t(m1), Q_{sop}^t(m1), Q_{sop}^t(m2), |V^t(1)|\}$. The equality constraints are met by running a distribution power flow (i.e., losses are considered at this stage). If a control variable hits the lower or upper bound, the control variable is fixed to the bound being violated. Inequality constraints are handled using a penalty function method. More on PSO is available in [12]. The upper and lower bounds of objectives used in the FMF are obtained from individual optimization results. The algorithm can be understood from algorithm 1.

IV. Test system and simulation studies

A. Test System

The numerical studies are carried out on the modified sixty-nine (69) bus medium voltage radial distribution network. It is modified to incorporate RES, residential and public EVCS. The base voltage and the base power of the system are 12.66 kV and 1 MVA, respectively. The network and load data are available in [13]. Forty-eight (48) SPGS units, each with an installed capacity of 48 kW, are dispersed across the network. Also, forty-eight (48) WPGS units, each of 200 kW capacity, are spread across the distribution network. The locations of the RES units have been adopted from [14]. There are thirty (30) residential EVCS in the network, locations of which are detailed in [14]. Each residential EVCS is equipped with "Standard-Type 2" chargers [14], and there are ten (10) charging outlets, each of capacity 22 kW. In other words, the total capacity of each residential EVCS is (10×22) kW $= 220$ kW. On the other hand, each public EVCS uses a fast charger of 50 kW rating [14]. Each public EVCS has six (6) outlets, i.e., the total capacity of each public EVCS is 6×50 kW $= 300$ kW. There are seventeen (17) EVCS in the distribution network, locations of which are adopted from [14]. Also, an SOP of 2.0 MVA rating is connected between the buses 25 and 26 [15]. The hourly profile of electrical load demands, RES generation, residential and public EV charging requirements have also been adopted from [14]. The hourly prices of grid power and demand response participation are shown in Fig. 1a. 10% loads are considered flexible. The loss in the SOP is considered 2%. Lines $\#1-\#8$, $\#17-\#23$, $\#31-\#39$, and $\#52-\#57$ are rated for 337.50 A. Other lines are rated for 260 A.

TABLE I
Summary of results

Details	Scenarios					
	S0	S1	S2	S3	S4	S5
Daily Energy loss (MWh)	4.018	3.888	3.888	4.103	3.888	4.095
Daily Operating Cost (INR in Lakhs)	3.1	2.904	2.904	2.917	2.904	2.917
Avg of min VSI in a day (pu)	0.765	0.958	0.958	0.837	0.958	0.888
Avg of AVD in a day (p.u.)	0.023	0.036	0.036	0.021	0.036	0.03
Avg of max line loading in a day (%)	51.97	51.46	51.46	52.96	51.46	52.6

B. Simulation Results

The following case studies/scenarios are considered:

- *Base case/Scenario S0*: In the base case scenario, DR implementation, and controls of SOP and ST are not considered. All other scenarios are compared with the base case.
- *Scenario S1*: The objective is to minimize the daily cost of operation using DR, SOP, and ST coordination.
- *Scenario S2*: The objective is to improve the VSI using DR, SOP, and ST coordination.
- *Scenario S3*: The objective is to minimize the AVD using DR, SOP, and ST coordination.
- *Scenario S4*: The objective is to minimize the line loading using DR, SOP, and ST coordination.
- *Scenario S5*: Combined objective using DR, SOP, and ST coordination.

The results for different scenarios are summarized in table I. The optimal settings of the SOP and the ST in different scenarios are shown in Fig. 2 and Fig. 3, respectively. The hourly profiles of electrical load, residential and public EVCS loads before and after implementation of the DR program are shown in fig.1b, fig.1c, and fig.1d, respectively. It is observed that the electrical demand and charging power profile for public EVCS are shifted to the period between hours $\#11$ to $\#17$. The peak of the residential EVCS is between hours $\#18$ and $\#22$. From table I, it is noted that the reduction in daily operating cost in scenario S1 is $\sim 6.32\%$. Similar figures are also noted in scenarios S2 (VSI improvement) and S4 (line loading reduction). The reduction in daily operating cost in scenario S3 (reduction of AVD) is $\sim 5.91\%$. In scenarios S1, S2, and S4, the load-side converter of the ST is set to 1.05 p.u. Therefore, the distribution network has comparatively higher bus voltages leading to lower line currents, lower losses, and improved VSI. Since the active power loss is reduced, the power drawn from the substation bus also decreases, resulting in a lower energy cost. From table I, it is also noted that the energy loss, operating cost, and VSI figures are similar in scenarios S1, S2, and S4. Therefore, objectives S1, S2, and S4 are aligned. Improvement in one of the three objectives improves the other two objectives. Compared to the base case scenario, the loss reduction is $\sim 3.23\% - 3.24\%$, the improvement in VSI is $\sim 6.32\%$, and the reduction in line loading is $\sim 0.97\%$ in scenarios S1, S2, and S4. Since the load side converter of the ST is set to 1.05 p.u., voltages at many buses exceed the nominal value of 1.00 p.u. Therefore, the AVDs are more in scenarios S1, S2, and S4 compared to the base case scenario S0. Therefore, an attempt to reduce the cost, improve the VSI, or reduce the line loading will increase the AVD.

The objective in scenario S3 is to minimize the AVD, i.e., to keep the bus voltages close to the nominal value of 1.00 p.u.

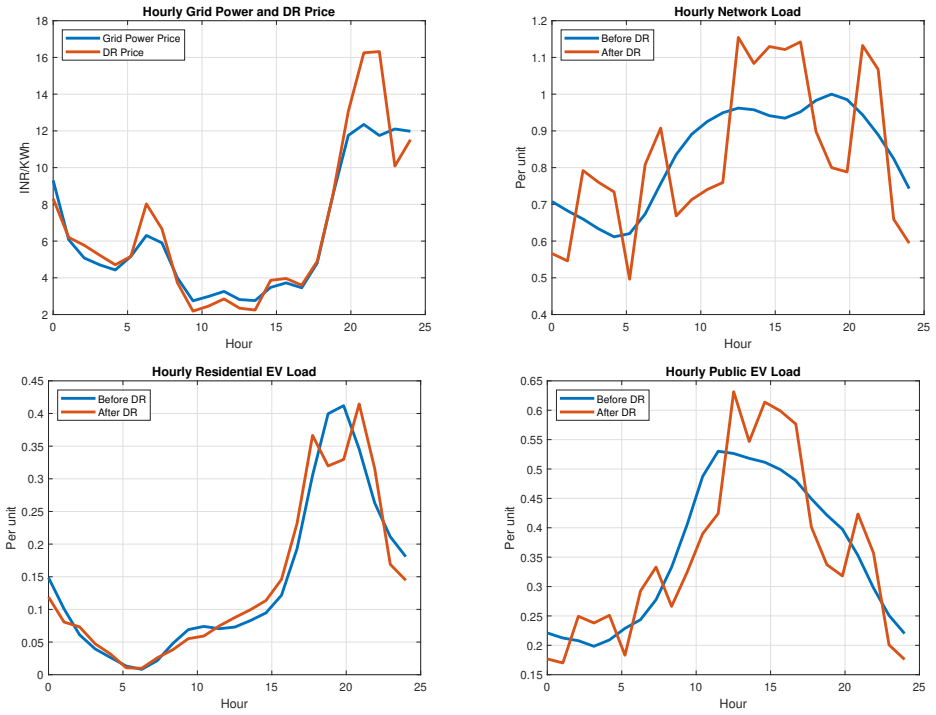

Fig. 1. Hourly Price and Load Profiles (a) Hourly Grid Power and DR Price (b) Hourly Network Load (c) Hourly Residential EV Load (d) Hourly Public EV Load

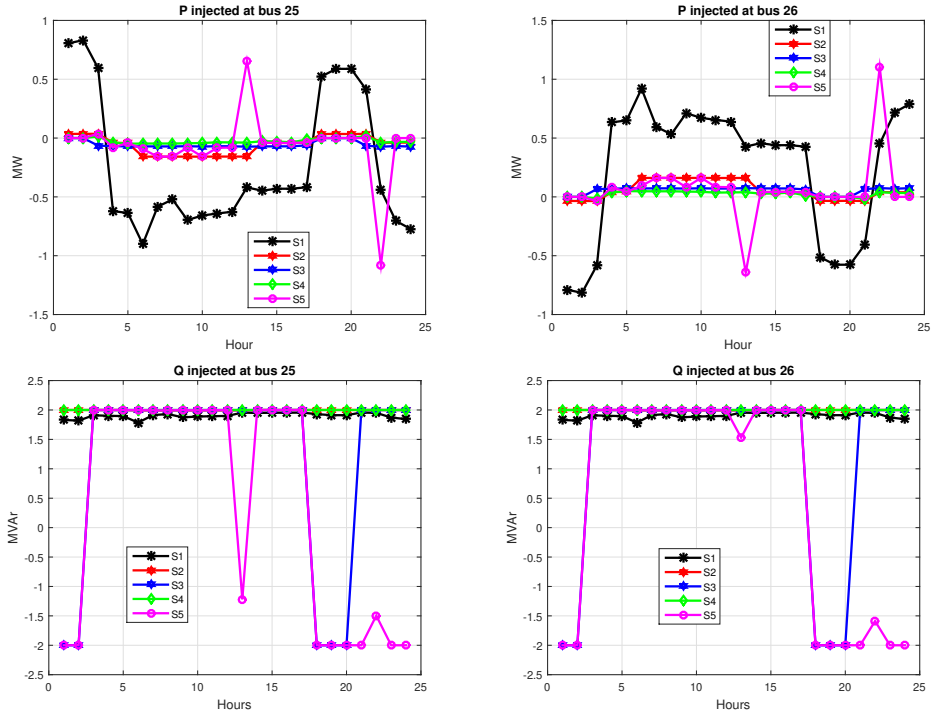

Fig. 2. SOP settings in different scenarios

It is observed that the ST setting changes hourly to realize the objective. However, the ST setting is never 1.05 p.u. Therefore, compared to scenarios S1, S2, and S4, the bus voltages are lower. It increases line loadings, active power loss, and energy costs (see table I). Further, the VSI becomes comparatively poor (see table I). The AVD reduces by $\sim 9.80\%$ compared to the base case (i.e., scenario S0). Therefore, objective S3 contradicts the requirements of objectives S1, S2, and S4. Therefore, an attempt to reduce the AVD will increase the operating cost and line loading and reduce the VSI.

Multi-objective optimization is solved in scenario S5, where all four objectives are to be met simultaneously. A compromise solution is needed in this scenario. From table I, it is observed that the cost reduction is $\sim 5.92\%$, the VSI improves by $\sim 16.08\%$, while the AVD and line loading deteriorates slightly. The authors also have verified that the solution of the

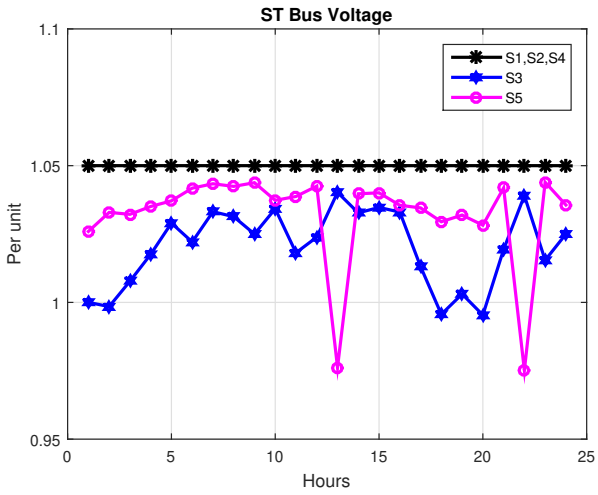

Fig. 3. Setting of the ST

multi-objective optimization obtained by the proposed method by comparing with "controlled elitist multi-objective genetic algorithm". The optimal solutions are found to be on the Pareto front.

V. Conclusions

A multi-objective EMS is proposed for an active distribution network to simultaneously minimize the cost of operation, improve the voltage stability, minimize the AVD, and reduce the line loadings. The distribution network comprises SPGS and WPGS, SOP, and ST. Moreover, residential and public EVCSs are also energized from the distribution network. A section of the electrical demand and residential and public EVCSs provide flexibility to the DSO by participating in the DR program. The DR scheduling is coordinated with the optimal setpoints of the SOP and the ST to meet the desired objectives. The multi-objective optimization problem is mapped to the fuzzy domain and solved using the minimum Euclidian distance to the utopia point approach. The optimization is carried out in two stages: linear programming and particle swarm optimization. The proposed algorithm has been validated on the modified version of the sixty-nine-bus radial distribution system. Simulation studies reveal that the operating cost can be reduced by $\sim 5.92\%$, and the VSI improves by $\sim 16.08\%$. However, reducing costs and improving the VSI causes slightly higher line loading and AVD.

References

[1] E. Dall'Anese, S. V. Dhople, and G. B. Giannakis, "Optimal dispatch of photovoltaic inverters in residential distribution systems," *IEEE Transactions on Sustainable Energy*, vol. 5, no. 2, pp. 487–497, 2014.

[2] H. Liang, J. Ma, and J. Lin, "Robust distribution system expansion planning incorporating thermostatically-controlled-load demand response resource," *IEEE Transactions on Smart Grid*, vol. 13, no. 1, pp. 302–313, 2021.

[3] V. C. Pandey, N. Gupta, K. R. Niazi, A. Swarnkar, and R. A. Thokar, "A hierarchical price-based demand response framework in distribution network," *IEEE Transactions on Smart Grid*, vol. 13, no. 2, pp. 1151–1164, 2021.

[4] V. B. Pamshetti and S. P. Singh, "Coordinated allocation of bess and sop in high pv penetrated distribution network incorporating dr and cvr schemes," *IEEE Systems Journal*, vol. 16, no. 1, pp. 420–430, 2022.

[5] P. Li, Z. Wang, J. Wang, W. Yang, T. Guo, and Y. Yin, "Two-stage optimal operation of integrated energy system considering multiple uncertainties and integrated demand response," *Energy*, vol. 225, p. 120256, 2021.

[6] R. You and X. Lu, "Voltage unbalance compensation in distribution feeders using soft open points," *Journal of Modern Power Systems and Clean Energy*, 2022.

[7] X. Wang, Q. Guo, C. Tu, L. Che, W. Yang, F. Xiao, and Y. Hou, "A two-layer control strategy for soft open points considering the economical operation area of transformers in active distribution networks," *IEEE Transactions on Sustainable Energy*, pp. 1–12, 2022.

[8] A. Singh and A. Maulik, "Energy management of distribution network in the presence of smart transformers, soft open points, and battery energy storage system," in *2022 International Conference on Power Energy Systems and Applications (ICoPESA)*, 2022, pp. 437–442.

[9] F. Sun, M. Yu, Q. Wu, and W. Wei, "A multi-time scale energy management method for active distribution networks with multiple terminal soft open point," *International Journal of Electrical Power & Energy Systems*, vol. 128, p. 106767, 2021.

[10] M. Chakravorty and D. Das, "Voltage stability analysis of radial distribution networks," *International Journal of Electrical Power & Energy Systems*, vol. 23, no. 2, pp. 129–135, 2001.

[11] H. A. Gabbar and A. Zidan, "Optimal scheduling of interconnected micro energy grids with multiple fuel options," *Sustainable Energy, Grids and Networks*, vol. 7, pp. 80–89, 2016.

[12] J. Kennedy and R. Eberhart, "Particle swarm optimization," in *Proceedings of ICNN'95-international conference on neural networks*, vol. 4. IEEE, 1995, pp. 1942–1948.

[13] D. Das, "A fuzzy multiobjective approach for network reconfiguration of distribution systems," *IEEE transactions on power delivery*, vol. 21, no. 1, pp. 202–209, 2005.

[14] A. Rabiee, A. Keane, and A. Soroudi, "Enhanced transmission and distribution network coordination to host more electric vehicles and pv," *IEEE Systems Journal*, 2021.

[15] Z. M. Ali, I. M. Diaaeldin, A. El-Rafei, H. M. Hasanien, S. H. Abdel Aleem, and A. Y. Abdelaziz, "A novel distributed generation planning algorithm via graphically-based network reconfiguration and soft open points placement using archimedes optimization algorithm," *Ain Shams Engineering Journal*, vol. 12, no. 2, pp. 1923–1941, 2021.